Dissecting the inner Galaxy with gamma-ray pixel count statistics

Silvia Manconi[1], Francesca Calore[2], Fiorenza Donato[3]

[1]Speaker, Institut für Theoretische Teilchenphysik und Kosmologie, RWTH Aachen University, Germany

[2]Univ. Grenoble Alpes, USMB, CNRS, LAPTh, F-74940 Annecy, France

[3]Dipartimento di Fisica, Università di Torino and Istituto Nazionale di Fisica Nucleare, Sezione di Torino, via P. Giuria, 1, I-10125 Torino, Italy

E-mail: `manconi@physik.rwth-aache.de`

Abstract. The nature of the GeV gamma-ray Galactic center excess (GCE) in the data of Fermi-LAT is still under investigation. Different techniques, such as template fitting and photon-count statistical methods, have been applied in the past few years in order to disentangle between a GCE coming from sub-threshold point sources or rather from diffuse emissions, such as the dark matter annihilation in the Galactic halo. A major limit to all these studies is the modeling of the Galactic diffuse foreground, and the impact of residual mis-modeled emission on the results' robustness. We combine for the first time adaptive template fitting and pixel count statistical methods in order to assess the role of sub-threshold point sources to the GCE, while minimizing the mis-modelling of diffuse emission components. We reconstruct the flux distribution of point sources in the inner Galaxy well below the Fermi-LAT detection threshold, and measure their radial and longitudinal profiles. We find that point sources and diffuse emission from the Galactic bulge each contributes about 10% of the total emission therein, disclosing a potential sub-threshold point-source contribution to the GCE.

1. Introduction

The Galactic center excess (GCE) is an unexpected γ-ray component detected at GeV energies from the inner degrees of the Galaxy in the data of the Large Area Telescope (LAT) aboard the *Fermi* satellite[1]. The GCE discovery raised a great interest in the community, and its nature is still under investigation. While the GCE morphology has been found to be consistent with a Navarro, Frenk and White (NFW) profile for annihilating particle dark matter (DM), see e.g. [2], it could also be due to a population of millisecond pulsars [3]. Stellar distributions were used as tracers of point sources (PS) emitting below threshold, and turned out to match the morphological features of GCE photons better than DM-inspired templates [4, 5, 6]. Complementary studies of photon-count statistics revealed initially that the GCE can be entirely due to a population of PS [7]. Recently, the DM interpretation was brought back [8], although hampered by systematics affecting photon-count statistical methods [9, 10, 11, 12].

A major limitation to all these studies is the modeling of the Galactic diffuse foreground, and the impact of residual mis-modeled emission on the results' robustness. As for template fitting methods, the analysis of the diffuse emission has been recently approached with the `skyFACT` algorithm, which fits the γ-ray sky by combining methods of image reconstruction and

adaptive spatio-spectral template regression [13]. The `skyFACT` method has been tested in the *Inner Galaxy* (IG) region, and probed to be efficient in the removal of most residual emission for a robust assessment of the GCE properties [13, 4].

Another source of uncertainty is the contribution of sub-threshold PSs. Photon-count statistical methods can discriminate photons from γ-ray sources based on their statistical properties. In particular, the 1-point probability distribution function method [14] (`1pPDF`) fits the contribution of diffuse and PS components to the γ-ray 1-point fluctuations histogram. Employing `1pPDF` on *Fermi*-LAT data, it was possible to measure the PS count distribution per unit flux, dN/dS, below the LAT detection threshold at high latitudes [14, 15, 16], and to set competitive bounds on DM [17].

We here apply the `1pPDF` method to *Fermi*-LAT data from the IG to understand the role of faint PS to the GCE, while minimizing the mis-modelling of diffuse emission components. To this end, we adopt a hybrid approach which combines, for the first time [18], adaptive template fitting methods as implemented in `skyFACT`, and `1pPDF` techniques.

2. Data and methods

We here summarize few aspects of the data and the methods used, while we refer to [18] for more details. We analyze 639 weeks of `P8R3 ULTRACLEANVETO` *Fermi*-LAT data until 2020-08-27. For the `skyFACT` fit we closely follow [4] and update the analysis for the increased data set and 4FGL catalog [19]. We follow a two-step procedure: First, we fit γ-ray data with `skyFACT` in order to build a model for the emission in the region of interest (ROI), maximally reducing residuals found to bias photon-count statistical methods [11]. Secondly, we run `1pPDF` fits with `skyFACT`-optimized diffuse models as input, and assess the role of PS to the GCE. We operate the `1pPDF` analysis in the energy range $2 - 5$ GeV [15, 17], restricting to events with best angular reconstruction (evtype=PSF3) and coming from the inner $20° \times 20°$, IG ROI hereafter. We cut at latitudes $|b| > 0.5°$ or $2°$ to check the stability of `1pPDF` results. Our goal being to quantify the role of PS to the GCE within the `1pPDF`, we add a *GCE smooth template* with free normalization in the `1pPDF` fit. As a baseline, we use the best-fit `skyFACT` bulge template in the `1pPDF` fit (`1pPDF-B`), and we define the `sF-B` diffuse model as the sum of best-fit inverse Compton, π^0 decay, *Fermi* bubbles, and extended sources, thus subtracting the bulge emission. The normalization, $A_{B/NFW126}$ for the bulge/NFW126 template, refers to the rescaling factor relative to the best-fit normalization from `skyFACT`. On the one hand, the use of `skyFACT` best-fit diffuse model guarantees a robust characterization of GCE spectrum and morphology against systematics related to the mis-modeling of the diffuse emission [11, 20], resolving over/under-subtraction issues by including a large number of nuisance parameters. On the other hand, the `skyFACT` optimization procedure mitigates possible systematics related to the mis-modeling of unaccounted components [9], by allowing spatial re-modulation in the fit templates. Besides the bulge, we also consider NFW126 as smooth GCE in the `1pPDF` analysis (`1pPDF-NFW126`). In this case, we construct the corresponding `skyFACT`-optimized diffuse model (`sF-NFW126`) from the `skyFACT` run adopting NFW126 as GCE, in analogy with the `sF-B` model. Finally, to bracket the uncertainties related to the optimization of the diffuse model, we also build a `skyFACT`-optimized diffuse template from the `skyFACT` run not including any GCE additional template (`sF-noGCE`).

3. Results

Inner Galaxy: skyFACT and 1pPDF fits. We first update the `skyFACT` analysis of the IG to the new *Fermi*-LAT dataset, confirming previous results [4, 5, 6]. A bulge distribution for GCE photons is strongly preferred by data on top of the NFW126-only model ($\sim 10\sigma$), and there is mild evidence for an additional NFW126 contribution on top of the bulge-only model ($\sim 4\sigma$).

We then use `skyFACT`-optimized diffuse and smooth GCE templates as input for `1pPDF` fits. Our results for a latitude cut of $2°$ are summarized in Fig. 1, where we show the best-fit dN/dS for
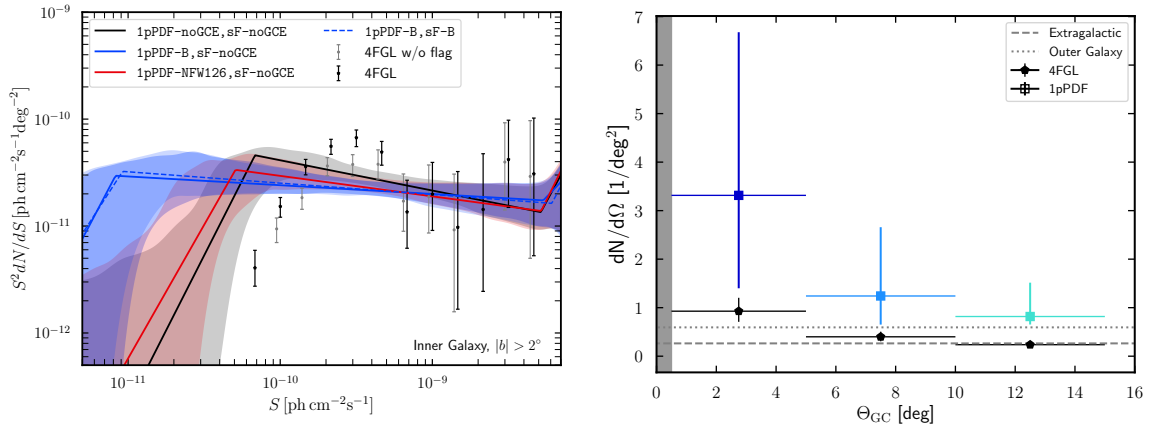
Figure 1. *Left: Source count distribution in the IG ROI* from the `1pPDF` fit for $|b| > 2°$. Solid (dashed) lines correspond to `sF-noGCE` (`sF-B`) diffuse template. The black line illustrates the `1pPDF-noGCE` case. The blue (red) line refers to `1pPDF-B` (`1pPDF-NFW126`) case. The colored areas correspond to 1σ uncertainty bands. The black (gray) points represent the count distribution of 4FGL sources (without any analysis flag, see [19]). *Right: Radial source density* $dN/d\Omega$ *profiles*, as reconstructed by the `1pPDF-B` fit using the `sF-B` diffuse model. We also display source density profiles for 4FGL sources (black points), and average source densities in the outer Galaxy and in the extragalactic ROIs.

the isotropic PS (IPS) in the IG ROI for several `1pPDF` fit configurations. In all fit setups shown, an IPS population is recovered below the LAT flux threshold. The reconstructed IPS dN/dS is stable against systematics related to the choice of `skyFACT`-optimized diffuse template, and latitude cut. Moreover, it does not present any spurious effect at the *Fermi*-LAT threshold ($\sim 10^{-10}$ ph cm^{-2} s^{-1}), and IPS are resolved down to $\sim 10^{-11}$ ph cm^{-2} s^{-1} for $|b| > 0.5°$, depending on the modeling of the smooth GCE component. This holds true even when no GCE smooth template is included neither in the `skyFACT` fit nor in the `1pPDF` one, contrary to what happens using non-optimized diffuse models [9, 11]. We therefore demonstrate, also in the context of `1pPDF` methods, that reducing large-scale residuals from mis-modeling of the diffuse emission improves the reconstruction of PS dN/dS.

We quantify now the evidence for models with an additional smooth GCE template using the Bayes factor. To this end, we compare the global evidence, $\ln \mathcal{Z}$, for the `1pPDF-noGCE`, `1pPDF-B` and `1pPDF-NFW126` setups, with different `skyFACT` diffuse model inputs, see Tab.1 in [18]. Regardless of the `skyFACT`-optimized diffuse template adopted, data *always* more strongly support models which include an additional smooth template for the bulge with respect to models without GCE in the `skyFACT` and/or `1pPDF` fits ($\ln B_{ij} > 20$), *and* models with an additional smooth NFW126 component in the `skyFACT` and/or `1pPDF` fits. Whenever a bulge template is included in our analysis, this is preferred even with respect to additional smooth DM templates. As for $|b| > 2°$, the evidence for an additional bulge template (`1pPDF-B`), with respect to `1pPDF-noGCE` is $\ln B \sim 95$. Models with PS *and* a smooth bulge component are therefore strongly preferred by data, regardless of the optimized diffuse model employed.

Characterizing the faint IPS component. Since the spatial distribution of PS is *isotropic* by construction, we test the PS spatial behavior by dissecting the IG ROI into three concentric annuli, masked for latitudes $|b| < 0.5°$. We extract the dN/dS separately in each ring, and integrate it over the flux interval $[10^{-11} - 10^{-9}]$ ph cm^{-2} s^{-1}. The result is reported in Fig. 1 as a function of the mean $\Theta_{GC} = \sqrt{b^2 + l^2}$ in each ring, for our baseline `1pPDF-B`, `sF-B` setup.
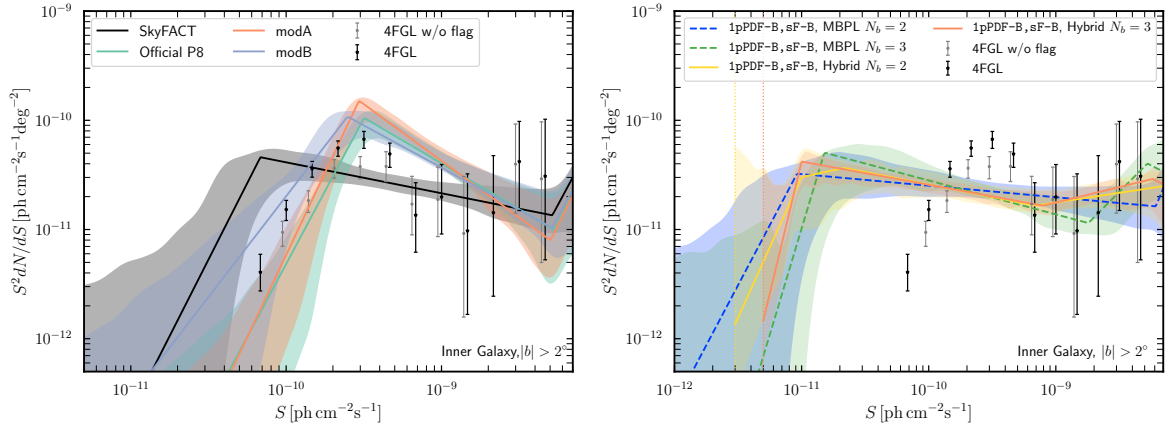
Figure 2. *Systematic for dN/dS reconstruction in the IG.* Source count distribution of the IG obtained from the 1pPDF analysis cutting the inner 2°. Left panel: Diffuse emission systematics. The black line is obtained from the `1pPDF` when using the model for the Galactic diffuse emission obtained from `skyFACT` (without any component modeling the GCE, `sF-noGCE`). The colored lines are instead obtained from the `1pPDF` using the official *Fermi*-LAT model for `Pass 8` (cyan line), or modA and modB (orange and indaco lines). Right panel: Effect of the number of free breaks N_b (dashed lines) and of the Hybrid fit approach with different number of breaks and varying the node position. The dotted line illustrates the position of S_{nd1} for the corresponding Hybrid fit.

We observe a decreasing trend of the $dN/d\Omega$ in the IG with Θ_{GC}. Also, the $dN/d\Omega$ in the innermost ring is about a factor of three higher than 4FGL sources, as well as than in OG and EG. For the most external ring, the source density is instead comparable with the catalog, and the density found in the outer and extragalactic sky. This corroborates the evidence that the IG PS population is *not purely isotropic nor extragalactic* in origin, but rather it peaks towards the GC. We also build the longitude profile of IG PS, see [18].

The `1pPDF` fits to *Fermi*-LAT data find non-null (and even comparable) emission from both the IPS population *and* the smooth GCE template, in most cases each contributing about 10% of the total emission in the ROI. Since 4FGL sources (2° cut, without analysis flag, see Fig. 1) account for 7% (10% including flagged sources) of the total IG emission, the remaining flux comes from sub-threshold IPS.

Systematics. The stability of the dN/dS results in the IG from the combined `1pPDF`-`skyFACT` analysis of *Fermi*-LAT data was tested against a number of systematics, including the ones from the diffuse emission templates and the dN/dS modeling, extensively discussed in [18]. We apply the `1pPDF` to the IG using other widely used diffuse emission templates: The official spatial and spectral template released by the *Fermi*-LAT Collaboration for `Pass 8` data (Official P8) (`gll_iem_v06.fits`, see Ref. [21]), and the models labeled A (modA) and B (modB), optimized for the study of the IGRB in [22]. By using standard diffuse models (modA, modB and Official P8), we reconstruct spurious sources at $\sim 4 \times 10^{-10}$ ph cm^{-2} s^{-1}, well above the sensitivity of the `1pPDF`, see Fig.2 (left panel). Such a peak of the IPS dN/dS disappears instead if we use diffuse emission templates as optimized with `skyFACT`. Large scale residuals are indeed reduced when allowing the spatial diffuse templates to be remodulated in the fit. Even in the absence of an additional GCE template, the `skyFACT` fit remodulates the diffuse components such to partially absorbs GCE photons, therefore reducing residuals and improving the fit with respect to standard diffuse models. We therefore confirm previous findings [11] that large residuals due to mis-modelling of diffuse emission induce a bias in the reconstruction of PS

in the inner Galaxy. We also verified that the an additional free break is not preferred by data, and that the MBPL obtained with three free breaks is compatible, within the uncertainties, with the case of two free breaks, see Fig. 2 (right panel). To test for possible effects connected to the faint end of the source-count distribution, we repeated the main analysis using the hybrid approach introduced in [14]. We set a fixed node at S_{nd1}, with the index of the power-law component below the last node, $n_f = -10$, thus effectively suppressing possible contributions in the ultra-faint regime below the fixed node. Results are summarized in the right panel of Fig. 2 for different values for the position of S_{nd1} in the faint source regime. To the extent we have tested, a node in the faint source regime at $3 - 5 \cdot 10^{-12}$ ph cm^{-2} s^{-1} does not affect the reconstructed dN/dS of the IG, which is well compatible, within 1σ uncertainty bands, with the benchmark results discussed in Fig. 1. In particular, the dN/dS is well compatible in the flux interval $10^{-11} - 10^{-9}$ ph cm^{-2} s^{-1} , where the radial and longitude profiles are computed.

4. Conclusions

Our results show that, within the statistical validity of the `1pPDF` and the setups tested, IPS and diffuse bulge each contributes about $\mathcal{O}(10\%)$ to the γ-ray emission along the lines-of-sight toward the GC. In particular, within our baseline model the `1pPDF` founds that PS (bulge) contribute 13% (10%) of the total emission of the IG. Subtracting the contribution from cataloged sources, a non-negligible fraction of the IG emission is accounted by sub-threshold PS. We also verified that this IPS population is not purely isotropic nor extragalactic in origin, rather it peaks towards the very GC. This further corroborates a possible, at least partial, stellar origin of the GCE.

References

[1] Murgia S 2020 *Ann. Rev. Nucl. Part. Sci.* **70** 455–483
[2] Calore F, Cholis I, McCabe C and Weniger C 2015 *Phys. Rev.* **D91** 063003 (*Preprint* 1411.4647)
[3] Abazajian K N 2011 *Journal of Cosmology and Astroparticle Physics* **1103** 010 (*Preprint* 1011.4275)
[4] Bartels R, Storm E, Weniger C and Calore F 2018 *Nature Astronomy* **2** 819–828 (*Preprint* 1711.04778)
[5] Macias O, Gordon C, Crocker R M, Coleman B, Paterson D, Horiuchi S and Pohl M 2018 *Nature Astronomy* **2** 387–392 (*Preprint* 1611.06644)
[6] Macias O, Horiuchi S, Kaplinghat M, Gordon C, Crocker R M and Nataf D M 2019 *JCAP* **09** 042 (*Preprint* 1901.03822)
[7] Lee S K, Lisanti M, Safdi B R, Slatyer T R and Xue W 2016 *Phys. Rev. Lett.* **116** 051103 (*Preprint* 1506.05124)
[8] Leane R K and Slatyer T R 2019 *Phys. Rev. Lett.* **123** 241101 (*Preprint* 1904.08430)
[9] Leane R K and Slatyer T R 2020 *Phys. Rev. Lett.* **125** 121105 (*Preprint* 2002.12370)
[10] Chang L J, Mishra-Sharma S, Lisanti M, Buschmann M, Rodd N L and Safdi B R 2020 *Phys. Rev. D* **101** 023014 (*Preprint* 1908.10874)
[11] Buschmann M, Rodd N L, Safdi B R, Chang L J, Mishra-Sharma S, Lisanti M and Macias O 2020 *Phys. Rev. D* **102** 023023 (*Preprint* 2002.12373)
[12] Leane R K and Slatyer T R 2020 *Phys. Rev. D* **102** 063019 (*Preprint* 2002.12371)
[13] Storm E, Weniger C and Calore F 2017 *JCAP* **08** 022 (*Preprint* 1705.04065)
[14] Zechlin H S, Cuoco A, Donato F, Fornengo N and Vittino A 2016 *Astrophys. J. Suppl.* **225** 18 (*Preprint* 1512.07190)
[15] Zechlin H S, Cuoco A, Donato F, Fornengo N and Regis M 2016 *Astrophys. J. Lett.* **826** L31 (*Preprint* 1605.04256)
[16] Manconi S, Korsmeier M, Donato F, Fornengo N, Regis M and Zechlin H 2020 *Phys. Rev. D* **101** 103026 (*Preprint* 1912.01622)
[17] Zechlin H S, Manconi S and Donato F 2018 *Phys. Rev. D* **98** 083022 (*Preprint* 1710.01506)
[18] Calore F, Donato F and Manconi S 2021 (*Preprint* 2102.12497)
[19] Abdollahi S *et al.* (Fermi-LAT) 2020 *Astrophys. J. Suppl.* **247** 33 (*Preprint* 1902.10045)
[20] Calore F, Cholis I and Weniger C 2015 *JCAP* **03** 038 (*Preprint* 1409.0042)
[21] Acero F *et al.* 2016 *ApJS* **223** 26 (*Preprint* 1602.07246)
[22] Ackermann M *et al.* 2015 *ApJ* **799** 86 (*Preprint* 1410.3696)